

# Magnetism, Spin Texture, and In-Gap States: Atomic Specialization at the Surface of Oxygen-Deficient SrTiO<sub>3</sub>

Michaela Altmeyer,<sup>1</sup> Harald O. Jeschke,<sup>1</sup> Oliver Hijano-Cubelos,<sup>2</sup> Cyril Martins,<sup>2</sup> Frank Lechermann,<sup>3,4</sup> Klaus Koepnik,<sup>5</sup> Andrés F. Santander-Syro,<sup>6</sup> Marcelo J. Rozenberg,<sup>2</sup> Roser Valentí,<sup>1</sup> and Marc Gabay<sup>2</sup>

<sup>1</sup>*Institute of Theoretical Physics, Goethe University Frankfurt am Main, 60438 Frankfurt am Main, Germany*

<sup>2</sup>*Laboratoire de Physique des Solides, Bat 510, Université Paris-Sud, 91405 Orsay, France*

<sup>3</sup>*I. Institut für Theoretische Physik, Universität Hamburg, 20355 Hamburg, Germany*

<sup>4</sup>*Institut f. Keramische Hochleistungswerkstoffe, TU Hamburg-Harburg, D-21073 Hamburg, Germany*

<sup>5</sup>*IFW Dresden Helmholtzstraße 20, 01069 Dresden, Germany*

<sup>6</sup>*CSNSM, Univ. Paris-Sud, CNRS/IN2P3, Université Paris-Saclay, Bât. 104 et 108, 91405 Orsay, France*

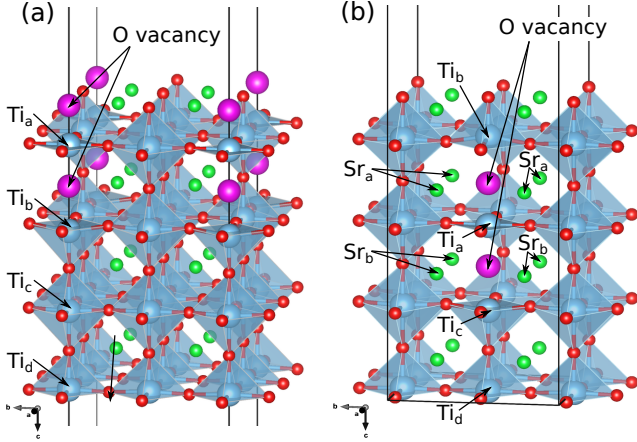


FIG. 1. SrO terminated  $2 \times 2 \times 4$  slab with two apically positioned oxygen vacancies (a) at the surface and (b) buried in the slab.

## I. SRO TERMINATED $2 \times 2 \times 4$ SLABS WITH OXYGEN DIVACANCIES

For completeness, we present here the results on the electronic and magnetic properties for further slabs considered in our study [Fig. 1]; an SrO-terminated  $2 \times 2 \times 4$  slab with a vertically placed surface divacancy and a SrO-terminated  $2 \times 2 \times 4$  slab with a divacancy buried inside the slab.

Our analysis of the single-vacancy SrO terminated  $2 \times 2 \times 4$  slab in the main text has already shown the presence of an in-gap state at  $\sim -0.4$  eV [Fig. 2(b), main text] of  $d_{z^2}$  character that originates from the Ti atom closest to the vacancy. Here we explore the effects of an additional vacancy in the slab located on the opposite side of this Ti atom [Fig. 1 (a)], as we would expect this additional vacancy to shift the in-gap states to higher binding energies. Furthermore, we also analyze the case, where this apically ordered divacancy is embedded in the slab [Fig. 1 (b)].

Note, that while the slabs considered in the main text (monovacancy  $2 \times 2 \times 4$  and divacancy  $3 \times 3 \times 4$ ) include O vacancy concentrations that are compatible with experimental estimates as discussed there, a divacancy in

a  $2 \times 2 \times 4$  slab, as considered in this Suppl. Inf. may correspond to a carrier concentration slightly above realistic values. The observations in actual measurements can therefore be expected to be a lot less drastic than the results presented in this section.

In Fig. 2 we present the relativistic nonmagnetic GGA+SO and ferromagnetic GGA+SO+U spin texture calculations for the two slabs in Fig. 1. As also found in the slabs considered in the main text, the nonmagnetic calculations [Figs. 2 (a) and (d)] show a characteristic Rashba spin texture with splittings of only a few meV.

In the magnetic calculations in a ferromagnetic  $m \parallel \hat{z}$  setup we find the same trends as observed in the slabs of the main text; i.e. an atomic specialization with in-gap states [Figs. 2 (b) and (e)] originating from Ti located in the immediate vicinity of the divacancy [ $\text{Ti}_a$  in Fig. 1] and spin winding at the Fermi surface with a small in-plane component [Figs. 2 (c) and (f)].

Three comments are in order: (i) All in-gap states obtained for the SrO-terminated  $2 \times 2 \times 4$  slabs are of  $d_{z^2}$  nature [Figs. 3 and 4]. Please note that the in-gap states in the  $3 \times 3 \times 4$  slab in the text correspond to a very special  $\text{TiO}_2$  surface arrangement of the vacancies. (ii) We observe that the position of the  $e_g$  in-gap states is very sensitive to the position and nature of the divacancy, as already commented in the main text. While the in-gap states lie at -1 eV in the slab with surface divacancies, it lies at -0.6 eV in the slab with the divacancies buried inside the slab. (iii) Due to the small size of the slab, the magnetic moments induced by the introduction of charge through the two vacancies distributes to all Ti in the slab, so that not only the  $\text{Ti}_a$   $e_g$  in-gap states acquire large magnetic moments but also the itinerant  $t_{2g}$  states, yielding considerable spin splittings. This has as a consequence that not both the up and down spin textures are visible at the Fermi level [Figs. 2 (c) and (f)]. As mentioned above, these  $2 \times 2 \times 4$  divacancy slabs probably represent an unrealistically high vacancy concentration. Nonetheless, the results are instructive, especially concerning the in-gap states and the fact that in-gap states at the experimentally observed -1.3 eV energies come from clustered vacancies near the surface.

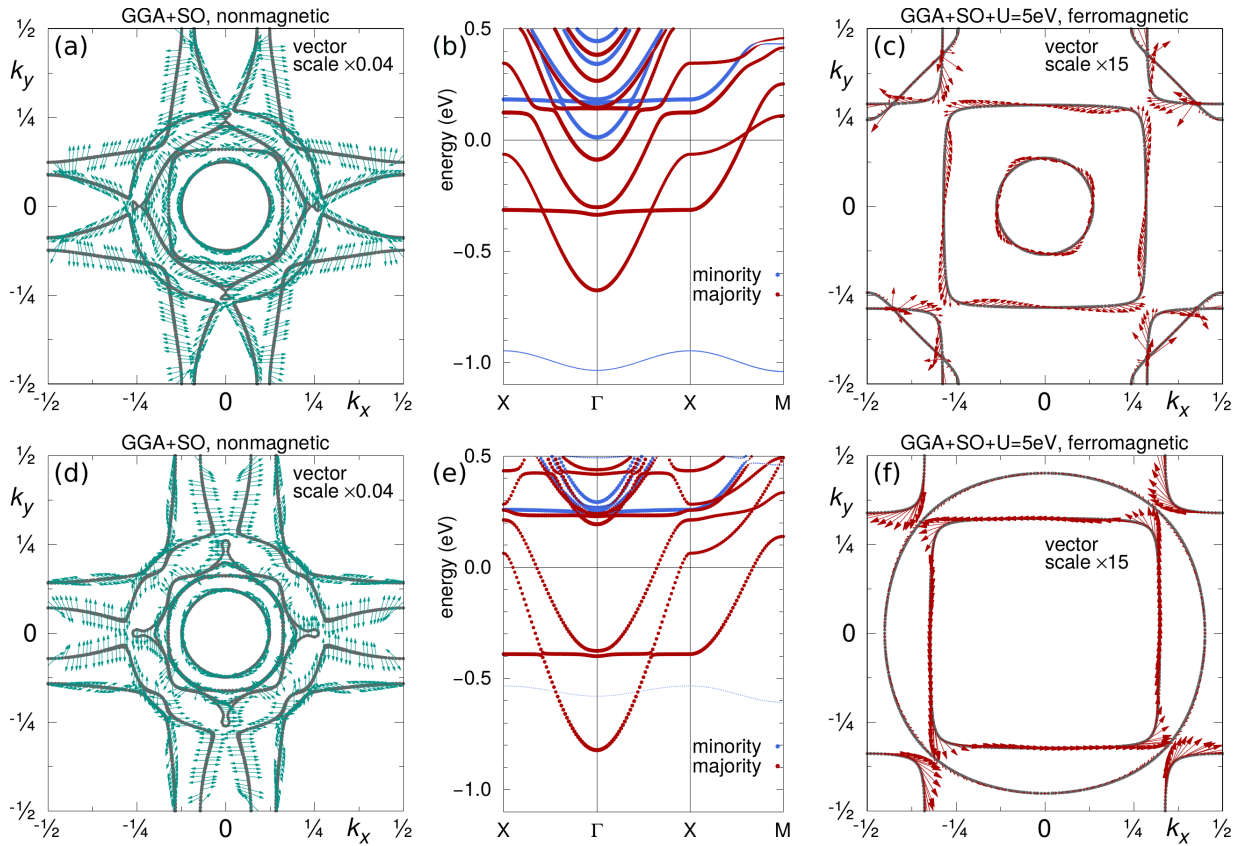


FIG. 2. Spin-textures and spin-polarized bandstructures for the relaxed  $2 \times 2 \times 4$  slabs with a divacancy (a)-(c) at the surface of the slab and (d)-(f) buried inside the slab.

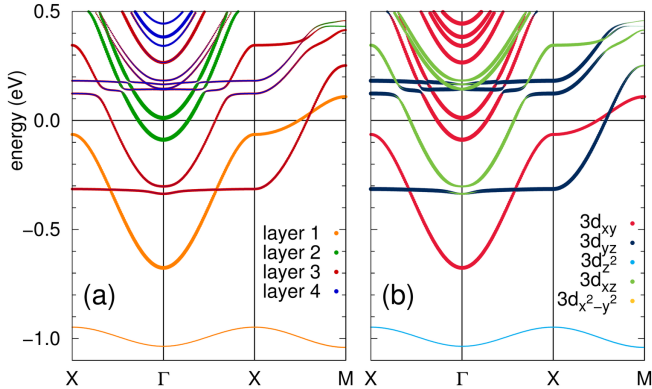


FIG. 3. Ferromagnetic GGA+SO+U Ti  $3d$  bandstructure for the relaxed  $2 \times 2 \times 4$  slab with two oxygen vacancies at the surface of the slab with a  $m \parallel \hat{z}$  setup. (a) Layer resolved. (b) Orbital resolved.

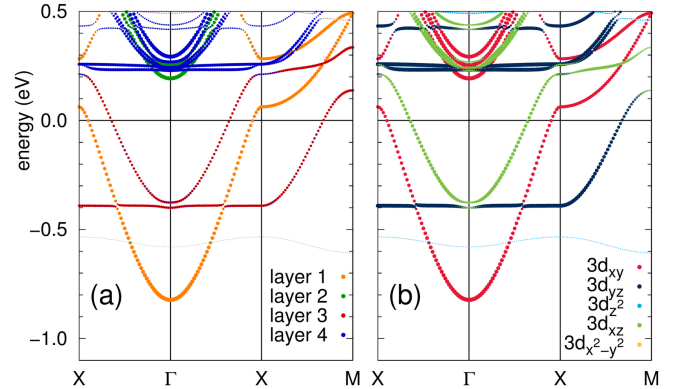


FIG. 4. Ferromagnetic GGA+SO+U Ti  $3d$  bandstructure for the relaxed  $2 \times 2 \times 4$  slab with two oxygen vacancies buried in the slab with a  $m \parallel \hat{z}$  setup. (a) Layer resolved. (b) Orbital resolved.

## II. DEPENDENCE OF THE CHOICE OF $U$ IN DFT CALCULATIONS ON $\text{SrTiO}_3$ SLABS

It is well known, that electronic correlations are typically underestimated in density functional theory (DFT). Hence, extensions of DFT like the “+ $U$ ” method used

in the present study have been established in the past. In the literature on  $\text{SrTiO}_3$  surfaces a few different values of  $U$  on the Ti  $3d$  orbitals have been considered. In our calculations presented in the main text of the paper we used a value of  $U = 5$  eV and a Hund’s coupling of  $J_H = 0.64$  eV. In order to test the robustness of our main statements we analyzed their sensitivity with respect to

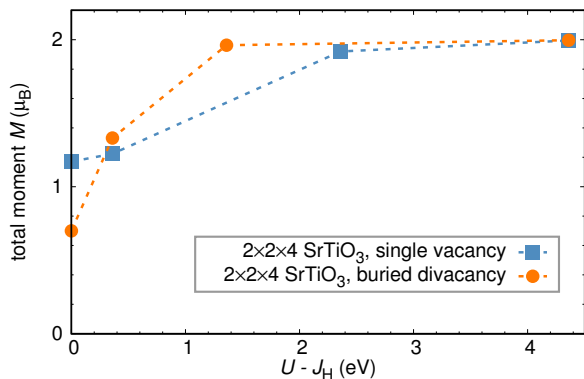


FIG. 5. Dependence of the total magnetic moment on the value  $U$  of the Hubbard interaction for SrO terminated  $2 \times 2 \times 4$  slabs with one or two vacancies.

changes in  $U$ .

In Fig. 5 we plot the total magnetic moment of the unit cell for two test cases (SrO terminated  $2 \times 2 \times 4$  slabs with one vacancy as shown in Fig. 1(a) of the main text and with a divacancy as shown in Fig. 1(b) of the supplement). Although the size of the magnetic moments reduces for smaller  $U$  values, it remains finite even down to  $U = J_H = 0$  eV. Moreover, a comparison of total energies shows that also in this case the magnetic state remains the ground state. In Fig. 6 we display the  $U$  dependence of the  $t_{2g}$ - $e_g$  resolved magnetic moments for the Ti atoms neighboring the vacancy for the single vacancy case presented in Fig. 1(a) of the main text. As expected, the overall trend shows a reduction of the magnetic moment on the neighboring Ti. Remarkably, the magnetic moment on  $Ti_d$ , which we found responsible for the observed giant spin splitting at the  $\Gamma$  point, is almost constant throughout the considered  $U$  range. This observation is further supported by calculations of the band structure [Fig. 7], where we compare the spin splitting corresponding to  $Ti_d$ . It does not appear to have a trivial dependence on  $U$ , but the order of the splitting remains compatible with the experimental values ( $\approx 50 - 100$  meV).

The fact that our main findings are present in GGA and GGA+ $U$  calculations demonstrates that recent worries about overestimation of spin splitting in some GGA+ $U$  functionals<sup>1</sup> do not affect our conclusions.

### III. CLUSTER CALCULATION

To gain further insight into the atomic and orbital specializations of the electronic states in the 2DES, we performed tight-binding calculations on  $2 \times 2 \times 4$  clusters where we only retain Ti  $3d$  and O  $2p$  states. For this structure there are a priori 472 such states, including spin. The O layer at the bottom is removed when we construct slabs containing an integer number of SrTiO<sub>3</sub> unit cells.

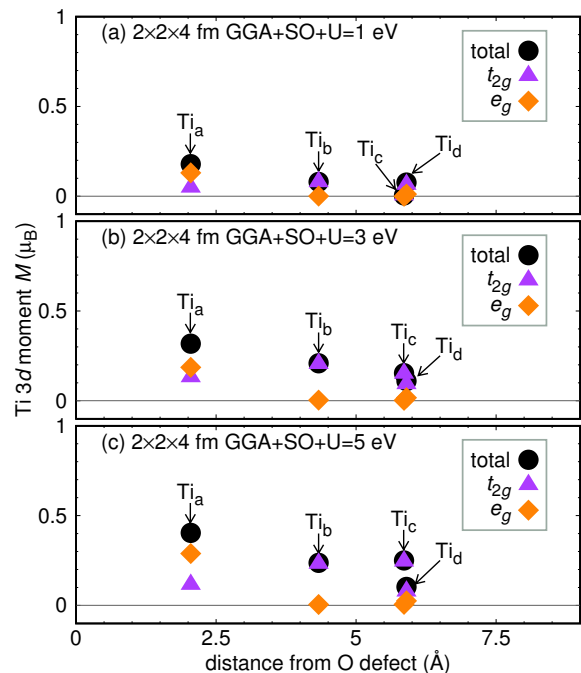


FIG. 6.  $t_{2g} - e_g$  resolved magnetic moments of the Ti atoms neighboring the monovacancy in the  $2 \times 2 \times 4$  SrO terminated slab (main text, Fig. 1(a)) for different values of the Hubbard repulsion parameter  $U$ .

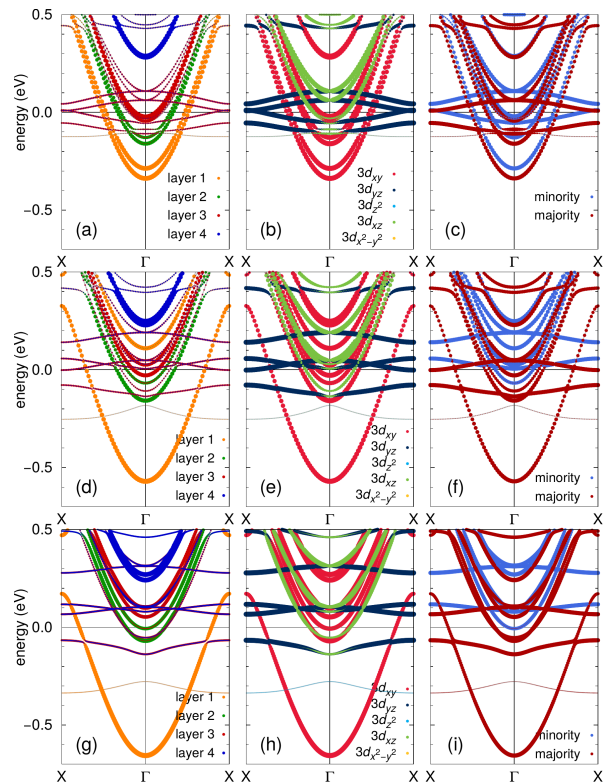


FIG. 7. Layer-, orbital and spin resolved band structure for the  $2 \times 2 \times 4$  slab with a single vacancy for Hubbard parameters of  $U = 1$  eV (a-c),  $U = 3$  eV (d-f) and  $U = 5$  eV (g-i).

We considered the following Hamiltonian:

$$H = H_o + H_{int} + H_{SO}$$

where

$$H_o = \sum_{i(\text{Ti})} \sum_d \sum_{\sigma=\uparrow,\downarrow} E_d a_{i(\text{Ti}),d,\sigma}^\dagger a_{i(\text{Ti}),d,\sigma} \\ + \sum_{j(\text{O})} \sum_p \sum_{\sigma=\uparrow,\downarrow} E_p b_{j(\text{O}),p,\sigma}^\dagger b_{j(\text{O}),p,\sigma}$$

$H_o$  is a diagonal matrix that contains the information of the on-site energies of the different atomic orbitals.  $a_{i(\text{Ti}),d,\sigma}^\dagger$  creates an electron in the Ti  $3d$  orbital at position  $i(\text{Ti})$ , with spin  $\sigma$  and  $b_{j(\text{O}),p,\sigma}^\dagger$  creates an electron in the O  $2p$  orbital at position  $j(\text{O})$  with spin  $\sigma$ .

Electronic site to site hops give rise to the kinetic contribution

$$H_{int} = \sum_{\langle i(\text{Ti}_1), j(\text{Ti}_2) \rangle} \sum_{d_1, d_2} \sum_{\sigma=\uparrow,\downarrow} T_{d_1, d_2, i(\text{Ti}_1), j(\text{Ti}_2)} \times \\ \times e^{i\mathbf{k}\cdot\mathbf{r}_{i(\text{Ti}_1)j(\text{Ti}_2)}} a_{i(\text{Ti}_1), d_1, \sigma}^\dagger a_{j(\text{Ti}_2), d_2, \sigma} \\ + \sum_{\langle i(\text{Ti}), j(\text{O}) \rangle} \sum_{d, p} \sum_{\sigma=\uparrow,\downarrow} T_{d, p, i(\text{Ti}), j(\text{O})} \times \\ \times e^{i\mathbf{k}\cdot\mathbf{r}_{i(\text{Ti})j(\text{O})}} a_{i(\text{Ti}), d, \sigma}^\dagger b_{j(\text{O}), p, \sigma} \\ + \sum_{\langle i(\text{O}_1), j(\text{O}_2) \rangle} \sum_{p_1, p_2} \sum_{\sigma=\uparrow,\downarrow} T_{p_1, p_2, i(\text{O}_1), j(\text{O}_2)} \times \\ \times e^{i\mathbf{k}\cdot\mathbf{r}_{i(\text{O}_1)j(\text{O}_2)}} b_{i(\text{O}_1), p_1, \sigma}^\dagger b_{j(\text{O}_2), p_2, \sigma} + h.c.$$

The most general case involves hops between neighboring titanium atoms (first term), between neighboring titanium-oxygen atoms (second term) and lastly between neighboring oxygen atoms (third term)<sup>2</sup>. Since the  $d$  and  $p$  orbitals are directional, hopping amplitudes depend on the relative positions and the orbitals of the two atoms involved in the path. Calculation of these amplitudes can

be done with the Slater-Koster rules<sup>3</sup> or can be obtained from a projection to Wannier functions of the DFT results.

$$H_{SO} = \lambda \mathbf{L} \cdot \mathbf{S}$$

$H_{SO}$  is the bulk spin-orbit coupling term. It lifts the spin degeneracy.

Values assigned to the various parameters are chosen such that in the absence of O vacancies the energy spectrum compares favorably with DFT calculations for slabs in the subspace of  $3d-2p$  states<sup>2</sup>.

Modeling an oxygen vacancy in the cluster is achieved by changing the on-site energy of the missing O, and the hopping amplitudes between the vacancy and the neighboring atoms. Furthermore, the presence of the missing oxygen may cause shifts in the positions of neighboring Ti atoms which in turn impact their on-site and kinetic contributions: locally the octahedral symmetry is broken and this changes the crystal field energy of the Ti  $3d$  orbitals; from ab initio calculations we know that the relative variation of the O-Ti-O bond angle for the shifted Ti is on the order of 3-4% and this affects the values of the local hopping amplitudes.

In order to monitor the evolution of the states in the presence of the vacancy, we adiabatically turn on the defect in the cluster, i.e. we incrementally change the different energy terms pertaining to the perturbation. We multiply these by a parameter  $\alpha$  which varies between 1 (no vacancy present) and 0 (vacancy present). In the case of a single vacancy in the topmost position of a SrO terminated cluster, we find that the distance between the emergent in-gap states and the conduction band bottom is  $\sim 0.42$  eV which compares well with the DFT results. For the same configuration, the orbital character of the in-gap state is of dominant  $d_{z^2}$  character. For a divacancy in the topmost SrO layer, an in-gap state with energy  $\sim -1.3$  eV is found.

<sup>1</sup> H. Chen, and A. J. Millis, Phys. Rev. B **93**, 045133 (2016).

<sup>2</sup> L. F. Mattheiss, *Energy Bands for KNiF<sub>3</sub>, SrTiO<sub>3</sub>, KMoO<sub>3</sub> and KTaO<sub>3</sub>*, Phys. Rev. B **6**, 4718 (1972).

<sup>3</sup> J. Slater and G. Koster, *Simplified LCAO method for the periodic potential problem*, Phys. Rev. **94**, 1498 (1954).